

Radar Communication for Combating Mutual Interference of FMCW Radars

Canan Aydogdu, Nil Garcia, Lars Hammarstrand, and Henk Wymeersch
Department of Electrical Engineering,
Chalmers University of Technology, Sweden
e-mail: canan@chalmers.se

Abstract—Commercial automotive radars used today are based on frequency modulated continuous wave signals due to the simple and robust detection method and good accuracy. However, the increase in both the number of radars deployed per vehicle and the number of such vehicles leads to mutual interference, cutting short future plans for autonomous driving and active safety functionality. We propose and analyze a radar communication (RadCom) approach to reduce this mutual interference while simultaneously offering communication functionality. We achieve this by frequency division multiplexing radar and communication, where communication is built on a decentralized carrier sense multiple access protocol and is used to adjust the timing of radar transmissions. Our simulation results indicate that radar interference can be significantly reduced, at no cost in radar accuracy.

I. INTRODUCTION

Automotive radar is becoming an indispensable equipment in modern cars, for different functions including adaptive cruise control and parking, especially due to its insensitivity to bad weather conditions [1]. Today, most automotive radar systems operate at 76–81 GHz [2], which provides good range resolution, on the order of centimeters [1] and the possibility to mitigate interference by locating the radars at different carrier frequencies [3]. Likewise, vehicle-to-vehicle (V2V) communication is becoming a standard, having proven its value in dissemination of safety critical information [1], [4]. However, both technologies have limitations related to the increased penetration rates. For example, current automotive radar sensors are not controllable or able to coordinate with sensors on other vehicles. Hence, mutual radar interference becomes a problem as in Fig. 1, resulting in increased noise floor [5], [6], in turn resulting in reduced detection capability and ghost detections [7].

Radar Communication (RadCom) is an approach to use radar hardware for communication purposes and can rely on the highly under-utilized frequency modulated continuous wave (FMCW) radar bandwidth. This idea was first applied in a vehicular application, where radar and communication signals are transmitted between a vehicle and a road side unit with a spread spectrum technique by two different chipping sequences [8]. Most of the other works consider orthogonal frequency division multiplexing (OFDM) for radar communications [9]–[11]. OFDM is widely used for communication due to its high degree of flexibility, low receiver complexity, and high performance under different propagation conditions.

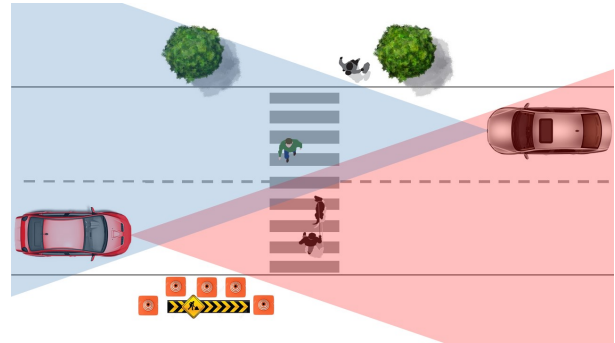


Fig. 1. Scenario with two vehicles in each other's field of view, leading to mutual interference.

The signal processing aspects of OFDM based RadCom is identified with its potential optimizations in [12]–[14] together with experimental test measurements to prove its applicability. An important challenge is that standard communication frequencies, such as the 5.9 GHz ISM band are generally unsuitable for radar, as the achieved accuracy and resolution is insufficient to meet automotive requirements [14]. In higher frequencies, a preliminary study for joint mmWave RadCom for a vehicular environment in the 60GHz band [15], used the IEEE 802.11ad preamble as a radar signal with standard WiFi receiver algorithms. This technique is shown to achieve a reasonable range and velocity estimation accuracy (0.1m and 0.1m/s). A similar study demonstrated how automotive sensor data is beneficial to the mmWave beam alignment, pointing out the possibility of adding mmWave communication functions on existing mmWave automotive radars in the 76-81 GHz band [16].

In this paper, we propose and analyze a novel RadCom approach for high-frequency FMCW radars, in which we repurpose a small part of the radar bandwidth to create an 802.11p-like V2V connection. The V2V channel is controlled via a carrier sense multiple access (CSMA) protocol and is utilized to control the timing of the radar signals. Vehicles are assumed to perform μ s-level clock synchronization with GNSS. We have performed an in-depth simulation of the proposed concept for a two-vehicle scenario. We find that under realistic propagation conditions, RadCom can significantly reduce the radar interference, with no performance degradation in terms of radar accuracy.

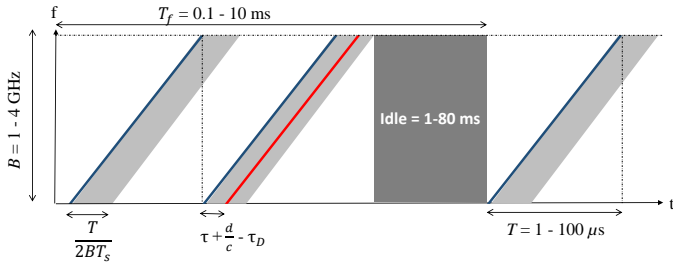


Fig. 2. FMCW modulation used in most automotive radar, with typical operating parameters. For a single radar, much of the time-frequency space is not utilized (the idle time is not shown to scale). The red line represents an interfering radar signal from another vehicle.

II. SYSTEM MODEL

A. FMCW Transmitter

We consider a sequence of frequency modulated continuous waves, i.e., chirps, transmitted by an FMCW radar, of the form

$$s(t) = \sqrt{P_{\text{tx}}} \sum_{k=1}^N c(t - kT) \quad (1)$$

where $c(t)$ is a chirp of the form $c(t) = \exp(j2\pi(f_c + Bt/T)t)$, P_{tx} is the transmit power, B denotes the radar bandwidth (typically 1–4 GHz), f_c is the carrier frequency (77 GHz), T is the chirp duration, and N is the number of chirps per frame. The frame time T_f comprises NT plus the idle and processing time. Depending on the maximum detectable range (d_{max}) and maximum detectable relative velocity (v_{max}), plus range and velocity resolution of the FMCW automotive radar, T , T_f and N take typical values seen in Fig. 2. In Fig. 2 the signal format (frequency occupancy as a function of time) of a sawtooth FMCW signal is shown, where the blue line is the transmitted chirp, the grey band corresponds to the sampling bandwidth of the receiver and the red line is an interference received from a FMCW radar which started transmission with a τ time difference. After N successive chirps, there is a significant idle time used for processing the samples. Further, the white region indicates a large fraction of unused time-frequency resources.

B. FMCW Receiver

At the co-located receiver, the backscattered signal is processed. The radar receiver comprises of the following blocks [17]: a mixer, an analog-to-digital convertor (ADC), and a digital processor. The mixer multiplies the received signal with a copy of the transmitted chirp. After low-pass filtering the resulting intermediate frequency (IF) signal, the mixer will output a signal with multiple harmonics at frequencies proportional to the time difference between the transmitted chirp and the received chirps. The output of the mixer is then sampled by the ADC, with sampling interval T_s , and passed to the digital processor which will detect and estimate the frequencies. The ADC bandwidth $1/(2T_s)$ is generally on the order of 10–50 MHz and is thus much smaller than B .

Considering a single target at distance d , the sampled backscatter signal, sample n or chirp k is of the form [1]

$$r_n^{(k)} = \sqrt{\gamma P_{\text{tx}} d^{-4}} \exp\left(j2\pi \frac{B(2d/c - 2\tau_D)}{T} nT_s\right) + w_n^{(k)} \quad (2)$$

where $\gamma = G_{\text{tx}}G_{\text{rx}}\sigma\lambda^2/(4\pi)^3$, for target radar cross section (RCS) σ , transmitter and receiver antenna gains G_{tx} and G_{rx} , Doppler time shift $\tau_D = Tv f_c/(Bc)$, in which c denotes the speed of light, v is the relative velocity between vehicles (note that a positive v corresponds to approaching vehicles and a positive Doppler shift, which leads to a decreased time difference between the transmitted and reflected radar signal), $w_n^{(k)}$ is additive white Gaussian noise (AWGN) with variance N_0 . A common approach to frequency retrieval in FMCW radar is to compute the fast Fourier transform (FFT) of the signal, average the signal through multiple chirp periods for enhanced SNR, and detect the peaks in the frequency-domain.

C. Goal

Our aim is to study the performance of the receiver when the target is itself a vehicle with an FMCW radar. We propose an FMCW-based RadCom system and investigate how the probability of mutual interference, the probability of false alarm and the ranging error are effected by the proposed scheme. This study focuses on resolving radar conflicts among vehicles with similar radar characteristics (same bandwidth and chirp signal), which is easier to analyze than the more general heterogeneous scenario.

III. RADAR INTERFERENCE ANALYSIS

In this section, we describe the interference model and calculate the conditions under which interference exists, both for a single link and for a network.

A. Interference Model

Consider the scenario in Fig. 1. Two cars with front-mounted FMCW radars facing each other approach a road-crossing where pedestrians are present. Both radars are FMCW based and use the same frequency band. If the interfering radar is located at distance d and has a relative delay τ between the ego vehicle transmission and the interfering vehicle transmission, then the received signal at the ego radar becomes

$$\tilde{r}_n^{(k)} = \begin{cases} r_n^{(k)} & \tau \notin V \\ r_n^{(k)} + \sqrt{\tilde{\gamma} P_{\text{tx}} d^{-2}} \exp\left(j2\pi \frac{B(\tau + d/c - \tau_D)}{T} nT_s\right) & \tau \in V \end{cases} \quad (3)$$

where $\tilde{\gamma} = G_{\text{tx}}G_{\text{rx}}\lambda^2/(4\pi)^2$ and V is the *vulnerable period* defined below.

Definition 1 (Vulnerable period V). *Given an ego vehicle radar that starts an FMCW transmission at time $t = 0$ and a facing vehicle radar with overlapping field-of-view that starts a transmission at time $t = \tau$, the vulnerable period V is the set of τ values for which interference to the ego vehicle radar occurs.*

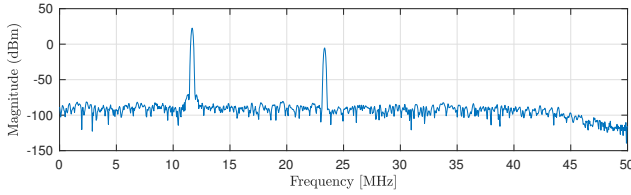


Fig. 3. FFT of received signal, with a interfering vehicle target at 70 m (23.33 MHz) and a ghost target at 35 m (11.67 MHz).

As illustrated in Fig. 2, the interfering signal transmitted by a time difference of τ is received at the ego radar at $\tau + d/c - \tau_D$. We note that interference has a factor d^{-2} while the useful signal has a factor d^{-4} , leading to an interference that is much stronger than the useful signal. Fig. 3 shows an example of such a received FMCW signal, for a vehicle target at distance 70 m from the radar, with $\tau = 0$, which in this case is in the vulnerable period. The target is observed at 23.33 MHz, whereas the strong interference is observed at 11.67 MHz, corresponding to 35 m.

B. Single Link Interference Condition

In this section, we will quantify the conditions under which interference occurs. The interfering transmission arrives at the ego vehicle with a propagation delay t_{prop} and a Doppler frequency shift of f_D . The Doppler shift is perceived by the ego vehicle as a delay $\tau_D = f_D T / B$ (see Fig. 2). Hence, the first received chirp at the ego vehicle starts at $t' = \tau + t_{\text{prop}} + \tau_D$ and interference will occur when $t' \in [0, T/(2BT_s)]$. If we further account for imperfect low-pass filtering at the ADC, which also causes mutual interference especially when the interference power is high, then interference will also occur when $t' \in [-T/(BT_s), -T/(2BT_s)]$. The maximum propagation delay of a received radar signal (not filtered out at the radar ADC) is $2d_{\text{max}}/c$, where d_{max} is the maximum detectable radar range and is related to chirp parameters by $d_{\text{max}} = cT/(4BT_s)$ [18]. Hence, the maximum propagation delay is $T/(2BT_s)$. The Doppler shift of an interfering signal is $\tau_D = \pm T v_{\text{max}} f_c / (Bc) = \pm 1/(4B)$ (approaching or receding), assuming that the maximum relative velocity of an interfering vehicle is equal to the maximum radar detectable relative velocity, given by $v_{\text{max}} = c/(4f_c T)$ [18]. Hence, the vulnerable period becomes

$$V = \left[-\frac{3T}{2BT_s} - \frac{1}{4B}, \frac{T}{2BT_s} + \frac{1}{4B} \right] \approx \left[-\frac{3T}{2BT_s}, \frac{T}{2BT_s} \right] \quad (4)$$

and is approximated due to $\tau_D \ll t_{\text{prop}}$ and $T_s \ll T$, resulting with approximated duration

$$|V| \approx \frac{2T}{BT_s}. \quad (5)$$

From this, it follows that the probability of interference for a single chirp is

$$P_{\text{int}}^{(c)} \approx \frac{|V|}{T} \approx \frac{2}{BT_s}. \quad (6)$$

However, a radar transmits during a fraction NT/T_f of the frame period and any interfering radar chirp sequence starting $(N-1)T$ prior up to the end of the radar transmission results with mutual interference due to overlapping of one or more chirps. Hence, the probability of interference for a frame for two facing radars is reduced to

$$P_{\text{int}}^{(f)} = \frac{(2N-1)T P_{\text{int}}^{(c)}}{T_f} \approx \frac{2NT P_{\text{int}}^{(c)}}{T_f}, \quad (7)$$

since for a typical automotive radar N is large.

Remark 1. Note that we have not accounted for reflections or additional targets in the environment. Such targets could also lead to interference. For that reason the vulnerable period could further be extended, following the same procedure as above. Additionally, if the radar has access to in-phase and quadrature samples, the vulnerable period can be reduced to $V \approx [-T/(2BT_s), T/(2BT_s)]$.

C. Network Interference Condition

For a network of vehicles, we first study a star topology around the ego vehicle. When there are M interfering vehicles, the probability of interference is $P_{\text{int}}^{(M)} = 1 - (1 - P_{\text{int}}^{(f)})^M$. For a more general topology with M vehicles, let \mathcal{G} be a directed radar graph with $\mathcal{G} = (\mathcal{V}, \mathcal{E})$, where each vertex corresponds to a radar $r_i \in \mathcal{V}$ and each edge $e_{ij} \in \mathcal{E}$ means that radar i is the field of view of radar j . The average probability of interference is then given by

$$\bar{P} = \frac{1}{|\mathcal{V}|} \sum_{r_i \in \mathcal{V}} P_{\text{int}}^{(M_i)} \quad (8)$$

where M_i denotes the number of edges into r_i .

D. Performance under Radar Interference

So-far we have only treated the probability of radar interference. When there is interference, we know from (3) that the interfering signal is generally stronger than the useful signal. This affects radar performance in a number of ways: it leads to ghost targets and an increase of the noise floor. Relevant performance metrics are thus the probability of detection, the probability of false alarm, and the ranging accuracy of the targets. These metrics will be analyzed in detail in Section V.

IV. RADCOM FOR INTERFERENCE REDUCTION

An FMCW-based-RadCom system is composed of three parts for sharing the wireless channel resource:

- 1) *Multiplexing* scheme for sharing among radar and communication,
- 2) *Radar MAC* scheme (rMAC) for coordination of radar sensing among different vehicles and
- 3) *Communication MAC* scheme (cMAC) for sharing among different vehicles.

In this study, we propose a RadCom scheme, where radar and communication are frequency division multiplexed (FDM) [19] with time division multiple access for radar signals (denoted rTDMA) and carrier-sense multiple access for communication signals (denoted cCSMA). The proposed RadCom

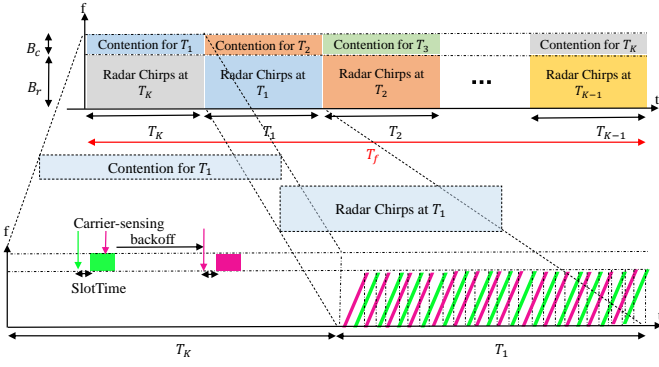


Fig. 4. RadCom scheme: FDM / rTDMA / cCSMA.

scheme uses communication in order to: (1) Disseminate non-overlapping rTDMA slots among radars to mitigate interference and (2) communicate data utilizing radar idle times. The focus of this article is the first function¹.

A. Multiplexing

Although multiplexing can be avoided by considering a joint waveform for communication and radar [13], such an approach is not suitable for automotive applications due to the limited ADC capabilities, which do not support full-band communication (e.g., OFDM) and modulating FMCW chirps would lead to extremely low data rates. Hence, we divide up the bandwidth B into a radar band B_r and a communication bandwidth B_c , for which $B_r + B_c \leq B$ and $B_c < 1/2T_s$, in order to be able to reuse the radar ADC.

B. Radar MAC

Facing FMCW radars operate interference-free if they are assigned non-overlapping rTDMA slots, which depend on the vulnerable duration. For this, vehicles are assumed to synchronize their clocks using GPS. Fig. 4 illustrates the division of the frequency-time domain for the proposed FDM/rTDMA/cCSMA based RadCom system. One radar frame duration T_f is divided into time slots T_i , where each radar transmits its chirp sequence during one T_i and remains idle during rest of the frame. One time slot T_i is of length $(N + 1)T$, which corresponds to the duration for sending N chirps plus one idle chirp time accounting for the overflow of time shifted rTDMA slots. This slotted time is set to provide non-overlapping chirp sequences and thereby maximize the number of vehicles with no mutual interference in the RadCom system, denoted by M_{\max} . Using the duration of the vulnerable period $|V|$ derived in (5), for the proposed rTDMA, at most $\lfloor T/|V| \rfloor$ different vehicle radars can coexist in a slot T_i and the maximum number of time slots per frame is $K = \lfloor T_f/(N + 1)T \rfloor$, which limits M_{\max} under perfect communication to

$$M_{\max} \leq K \lfloor T/|V| \rfloor \approx K \lfloor B_r T_s / 2 \rfloor. \quad (9)$$

¹The latter function is investigated in future studies and fully exploits FDM, whereas realization of the first function is based on frequency division.

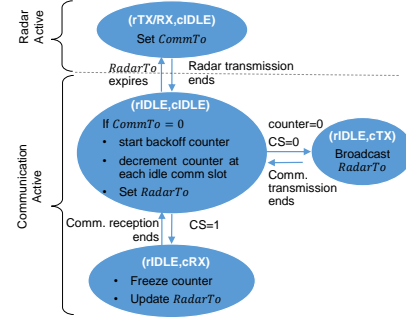


Fig. 5. State diagram for the proposed RadCom scheme.

C. Communication

V2V vehicular communication is used to assign non-overlapping rTDMA slots among facing vehicles. Since communication links are not necessarily symmetric due to the directivity of the radar, a best effort approach with no acknowledgements is employed. Communication during slot T_{i-1} determines the rTDMA slots in T_i as illustrated in Fig. 4. Each time slot T_i is further divided to slots called *SlotTimes*, which are used by the non-persistent CSMA mechanism. Communication packets are transmitted if the channel is sensed idle for one *SlotTime* or a random backoff is employed if channel is sensed busy. Each vehicle sequentially uses two timeouts: (1) Communication timeout (*CommTo*) for starting transmission of a communication packet and (2) Radar timeout (*RadarTo*) for starting the radar chirp sequence. A communication packet (which includes the *RadarTo* information) is transmitted upon expiration of *CommTo*, whereas the FMCW radar chirp sequence is transmitted upon expiration of *RadarTo*.

A state diagram for the proposed RadCom scheme is given in Fig. 5, where each state denoted by (rX, cY) corresponds to radar state X and communication state Y . Radar is active in $(rTX/RX, cIDLE)$ state and upon end of radar transmission the RadCom hardware enters $(rIDLE, cIDLE)$ state, where communication is active and carrier sensing is deployed. Upon expiration of *CommTo*, a backoff counter starts and decrements for each idle *SlotTime*. If carrier is sensed idle when the counter expires (*counter* = 0 and *CS* = 0), the state $(rIDLE, cTX)$ is entered, where the vehicle broadcasts its *RadarTo*. Otherwise if carrier is sensed busy, the state $(rIDLE, cRX)$ is entered (*CS* = 1), where reception takes place and any active backoff counters are frozen. In this state, the ego vehicle stores the received radar timeout values of other vehicles and updates its own *RadarTo* to be advertised according to the received radar timeout so as to use one of the left rTDMA slots in T_i or in T_{i+1} , etc. No measures are taken in case of communication failures and there remains a small probability for mutual interference with the RadCom scheme, which will be analyzed in a future study.

V. PERFORMANCE EVALUATION AND RESULTS

The performance of an FMCW receiver when the target is itself a vehicle with an FMCW radar is investigated. A

TABLE I
SIMULATION PARAMETERS.

Parameter	Value		
Radar	Chirp duration (T)	20 μ s	
	Frame duration (T_f)	20 ms	
	Time slots per frame (K)	10	
	Radar bandwidth	0.96 GHz–1 GHz	
	d_{\max} for $B_c = 0$	150 m	
	v_{\max}	140 km/h	
	P_{tx}	11 dB	
	SNR	10 dB	
	N	99	
	f_c	77	
	T_s	0.01 μ s	
	Chebyshev low-pass filter order	13	
	Thermal noise temperature	290 K	
	Receiver's noise figure	4.5 dB	
	Comm.	Communication bandwidth B_c	20 MHz, 40 MHz
		Packet size (N_{pkt})	4800 Bits
Modulation		16-QAM	
MAC		non-persistent CSMA	
SlotTime		10 μ s	
Backoff window size		6	

comparison is made by the proposed FMCW-based RadCom system in terms of the probability of false alarm and the ranging error. The probability of mutual interference and the necessary time to resolve contention for multiple vehicles are evaluated.

A. Simulation Parameters

The simulation parameters are summarized in Table I. Two facing vehicles are assumed to have radars with the same properties. Radar is FMCW with sawtooth waveform. The chirp sequence is designed so as to meet the maximum detectable relative velocity $v_{\max} = 140$ km/h, the maximum detectable range $d_{\max} = 150$ m when $B_c = 0$ (since it increases for RadCom), velocity resolution smaller than 1 m/s and range resolution of 15 cm. Radar front-end-hardware component parameters are taken as in [17]. The mean value for the radar cross section of a car is taken as 20 dBsm [17], [20]. At the signal processing stage, coherent pulse integration is applied. Moreover, a Blackman-Harris window to reduce the height of the sidelobes is applied before the FFT module. Finally, greatest of cell averaging constant false alarm rate (GoCA-CFAR) thresholding with 50 training cells with 2 guard cells is used for radar detection. The vulnerable duration for $B_c = 20$ MHz is computed to be $|V| = 4.17 \mu$ s (4), leading to maximum 4 concurrent radar transmissions per T_i , resulting with $M_{\max} = 40$ vehicles supported maximum by the proposed RadCom system.

B. Results

We first consider probability of the radar interference for a multi-vehicle scenario, and then evaluate the RadCom performance in terms of delay to resolve contentions. Finally, we present in-depth results for two vehicles, with and without RadCom.

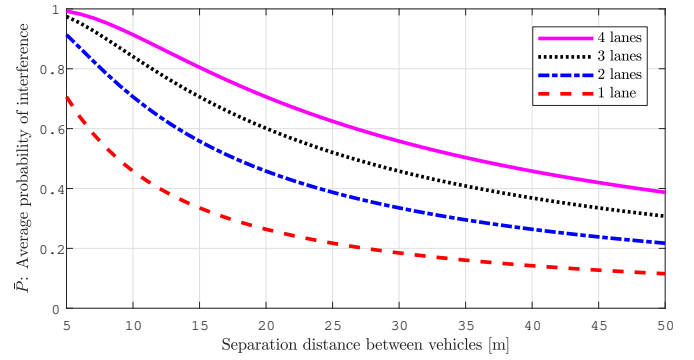


Fig. 6. Average probability of interference for varying vehicle separation distance and different number of lanes for $B_c = 20$ MHz.

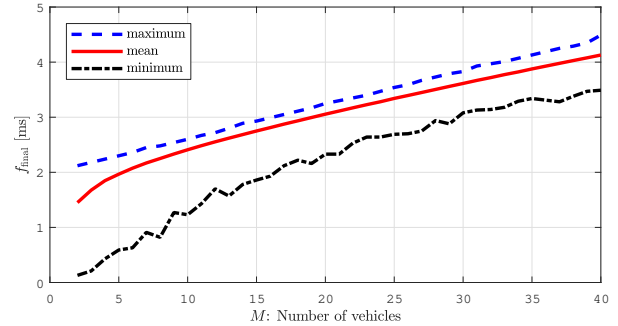


Fig. 7. Time necessary to resolve communication contention among M vehicles for $B_c = 20$ MHz.

1) *Radar Interference*: The average probability of interference, \bar{P}_i , for varying separation distance between vehicles on a lane and different number of lanes is given by Fig. 6 for $B_c = 20$ MHz. The average probability of interference increases by lower vehicle separation and higher number of lanes, i.e., increased density of vehicles. We conclude that for dense multi-lane traffic, radar interference is a grave concern, despite the low duty cycle.

2) *Communication Delay*: We denote the time to resolve contention among connected M vehicles by t_{final} . The vehicles apply non-persistent CSMA with random backoff. Based on 10,000 Monte Carlo runs, Fig. 7 shows the average, minimum, and maximum value of t_{final} as a function of M for $B_c = 20$ MHz. We assume that all M stations initiate transmission attempts during the time slot T_1 . We observe that the contention time for $M_{\max} = 40$ vehicles lasts up to 5 ms and is resolved within a radar frame, which is $T_f = 20$ ms. Hence, the proposed communication scheme is feasible and fast enough to allocate rTDMA slots to 40 vehicles before the radar frame ends. Furthermore, a larger communication bandwidth will lead to lower t_{final} leaving space for other types of communications.

3) *Radar Interference with RadCom*: The performance of RadCom is evaluated for the communication bandwidths $B_c \in \{20, 40\}$ MHz. The distance between two vehicles (d) and the time difference between starting times of chirps (τ) are

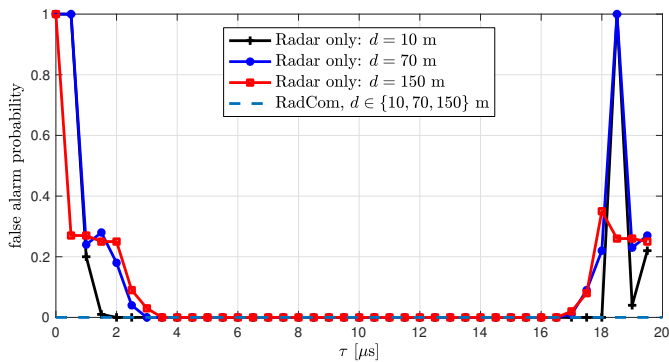


Fig. 8. Comparison of probability of false alarm between radar and RadCom with $B_c = 20$ MHz.

varied. The performance of radar only and RadCom schemes are compared in terms of probability of false alarm (P_f) and ranging error based on 100 Monte Carlo simulations. Fig. 8 shows the probability of false alarm without RadCom for $B_c = 20$ MHz for varying τ and three different d values. The transmissions during the vulnerable period V is observed to result with interference for especially $\tau < T/(2BT_s) = 1 \mu\text{s}$ and $\tau = 17\text{--}20 \mu\text{s}$, described in (4). False alarm probability increases with increasing d due to attenuated radar received signals. With RadCom, the false alarm probability is reduced to zero for all τ and d due to avoiding transmissions during the vulnerable period. Note that, RadCom has non-zero probability of false alarm even with RadCom, which is not observed due to the low number of simulations.

Simulations taken over varying τ and d , show that the ranging error is independent of τ and at most 6.9 cm, 7.4 cm and 8.54 cm for radar only, RadCom with $B_c = 20$ MHz and $B_c = 40$ MHz, respectively. While RadCom in theory can lead to an accuracy reduction due to reduced bandwidth, this effect is insignificant, since the relative decrease in radar bandwidth is negligible (at most 4%) and we operate in high SNR.

VI. CONCLUSION

We have evaluated a RadCom approach building on a combination of FDM, TDMA for radar, and CSMA for communication. The approach exploits the low utilization of time and frequency of a typical radar, as well as the limited impact of a small bandwidth loss on the radar performance. We have performed an interference analysis at both the link and network level and found that with higher penetration, interference is prevalent. With our proposed approach, we are able to mitigate interference by shifting radar transmissions in time. Performance in terms of false alarms, missed detections, and ranging accuracy are reported, based on high-fidelity simulations. Future work will consider larger-scale scenarios for heterogeneous FMCW radars with different bandwidths and chirp parameters, as well as the interference from multipath.

ACKNOWLEDGMENT

This work is supported, in part, by Marie Curie Individual Fellowships (H2020-MSCA-IF-2016) Grant 745706 (Green-

Loc) and a SEED grant from Electrical Engineering Department of Chalmers University of Technology.

REFERENCES

- [1] S. M. Patole, M. Torlak, D. Wang, and M. Ali, "Automotive radars: A review of signal processing techniques," *IEEE Signal Processing Magazine*, vol. 34, no. 2, pp. 22–35, 2017.
- [2] J. Hasch, E. Topak, R. Schnabel, T. Zwick, R. Weigel, and C. Waldschmidt, "Millimeter-wave technology for automotive radar sensors in the 77 GHz frequency band," *IEEE Transactions on Microwave Theory and Techniques*, vol. 60, no. 3, pp. 845–860, March 2012.
- [3] T. Schipper, M. Harter, L. Zwirello, T. Mahler, and T. Zwick, "Systematic approach to investigate and counteract interference-effects in automotive radars," in *IEEE 9th European Radar Conference*, 2012, pp. 190–193.
- [4] L. Kong, M. K. Khan, F. Wu, G. Chen, and P. Zeng, "Millimeter-wave wireless communications for IoT-cloud supported autonomous vehicles: Overview, design, and challenges," *IEEE Communications Magazine*, vol. 55, no. 1, pp. 62–68, January 2017.
- [5] M. Goppelt, H.-L. Blöcher, and W. Menzel, "Analytical investigation of mutual interference between automotive FMCW radar sensors," in *German Microwave Conference (GeMIC)*. IEEE, 2011, pp. 1–4.
- [6] A. Bourdoux, K. Parashar, and M. Bauduin, "Phenomenology of mutual interference of FMCW and PMCW automotive radars," in *IEEE Radar Conference (RadarConf)*, May 2017, pp. 1709–1714.
- [7] I. M. Kunert, "Project final report, MOSARIM: More safety for all by radar interference mitigation," 2012. [Online]. Available: <http://cordis.europa.eu/docs/projects/cnect/1/248231/080/deliverables/001-D611finalreportfinal.pdf>
- [8] M. Takeda, T. Terada, and R. Kohno, "Spread spectrum joint communication and ranging system using interference cancellation between a roadside and a vehicle," in *IEEE 48th Vehicular Technology Conference*, vol. 3, May 1998, pp. 1935–1939.
- [9] B. J. Donnet and I. D. Longstaff, "Combining MIMO radar with OFDM communications," in *European Radar Conference*, Sept 2006, pp. 37–40.
- [10] D. Garmatyuk, J. Schuerger, and K. Kauffman, "Multifunctional software-defined radar sensor and data communication system," *IEEE Sensors Journal*, vol. 11, no. 1, pp. 99–106, Jan 2011.
- [11] C. Sturm and W. Wiesbeck, "Waveform design and signal processing aspects for fusion of wireless communications and radar sensing," *Proceedings of the IEEE*, vol. 99, no. 7, pp. 1236–1259, July 2011.
- [12] P. Falcone, F. Colone, C. Bongioanni, and P. Lombardo, "Experimental results for OFDM wifi-based passive bistatic radar," in *IEEE Radar Conference*, May 2010, pp. 516–521.
- [13] C. Sturm, T. Zwick, W. Wiesbeck, and M. Braun, "Performance verification of symbol-based OFDM radar processing," in *IEEE Radar Conference*, May 2010, pp. 60–63.
- [14] L. Reichardt, C. Sturm, F. Grunhaupt, and T. Zwick, "Demonstrating the use of the IEEE 802.11p car-to-car communication standard for automotive radar," in *6th European Conference on Antennas and Propagation (EUCAP)*, March 2012, pp. 1576–1580.
- [15] P. Kumari, N. Gonzalez-Prelcic, and R. W. Heath, "Investigating the IEEE 802.11ad standard for millimeter wave automotive radar," in *IEEE 82nd Vehicular Technology Conference (VTC)*, Sept 2015, pp. 1–5.
- [16] J. Choi, V. Va, N. Gonzalez-Prelcic, R. Daniels, C. R. Bhat, and R. W. Heath, "Millimeter-wave vehicular communication to support massive automotive sensing," *IEEE Communications Magazine*, vol. 54, no. 12, pp. 160–167, December 2016.
- [17] C. Karnfelt, A. Paden, A. Bazzi, G. E. H. Shhade, M. Abbas, and T. Chonavel, "77 GHz ACC radar simulation platform," in *9th International Conference on Intelligent Transport Systems Telecommunications (ITST)*, Oct 2009, pp. 209–214.
- [18] M. I. Skolnik, *Radar Handbook*, 3rd ed. New York: McGraw-Hill Education, 2008.
- [19] H. Hellsten and P. Dammert, "Short range radar cohabitation: Extension to integrated communication," Saab Surveillance Report, 2017.
- [20] S. Lee, S. Kang, S. C. Kim, and J. E. Lee, "Radar cross section measurement with 77 GHz automotive FMCW radar," in *IEEE 27th Annual International Symposium on Personal, Indoor, and Mobile Radio Communications (PIMRC)*, Sept 2016, pp. 1–6.